

## Supporting Information

### **Spirobifluorene-based Conjugated Microporous Polymer Embedded with *N*-Hydroxyphthalimide as Synergistic Photocatalyst for Selectively Solvent-Dependent Aerobic Oxidations**

Tao Fan, Lei Fang, Ying Yin, Guocai Wu, Hui Xu, Liangchun Li\*

*Shanghai Key Lab of Chemical Assessment and Sustainability, School of Chemical  
Science and Engineering, Tongji University, 1239 Siping Road, Shanghai, 200092,  
China.*

\*Corresponding author: E-mail: [lilc@tongji.edu.cn](mailto:lilc@tongji.edu.cn)

## Contents

<b>1. General information</b> .....	1
<b>2. Experimental produces</b> .....	2
<b>3. Figures and tables</b> .....	4
<b>4. References</b> .....	10

## 1. General information

All reagents and solvents were used as received from commercial sources, unless otherwise specified, and used without further purification. Compound **4** was synthesized according to the literature [1].

UV-Vis absorption was recorded on a Shimadzu UV-1800 spectrophotometer. Solid-state  $^{13}\text{C}$  CP/MAS NMR spectrum was obtained by Bruker Avance Neo 400WB. Scanning electron microscopy (SEM) images were performed on a JEOL JSM-7900F instrument. Thermal gravimetric analysis (TGA) was conducted on a differential thermal analyzer (TA, Q500) by heating the samples from 30 °C to 600 °C with a heating rate of 10 °C min<sup>-1</sup> in N<sub>2</sub> atmosphere (60 mL min<sup>-1</sup>). The Brunauer-Emmett-Teller (BET) surface areas were measured using the Micromeritics TRISTAR. Fourier Transform Infrared (FT-IR) spectroscopy was recorded using a Nicolet iS20 FT-IR spectrophotometer in 4000–500 cm<sup>-1</sup> region. Gas adsorption measurements were conducted using the gas adsorption equipment TRISTAR 3020. The products of the aerobic oxidation reactions were analyzed by gas chromatography mass spectrometry (GC-MS, SHIMADZU GCMS-QP2010 SE W) using SH-Rxi-5Sil MS column. Electron Paramagnetic Resonance (EPR) spectra were carried out on Bruker A300-10/12 spectrometer set with the following experimental parameters: frequency, 9.824 GHz; power, 6.325 mW; modulation amplitude, 1.00 G; modulation frequency, 100 kHz; sweep time, 30.00 s; center field, 3500.00 G; sweep width, 100.0 G.

## 2. Experimental produces

**Photoelectrochemical measurements.** Mott Schottky and transient-state photocurrent were made in sodium sulfate solution (0.1 M, pH = 7) through the traditional three electrode system in the CHI 760E electrochemical workstation. The working electrode is ITO glass plate coated with catalyst slurry. The platinum foil is used as counter electrode and saturated Ag/AgCl is used as reference electrode.

**Preparation of working electrode.** 4 mg catalyst, 0.49 mL ethanol and 10  $\mu$ L Nafion were mixed and ultrasound for 10 min. And then, the slurry was deposited evenly on the ITO glass plate ( $2 \times 2 \text{ cm}^2$ ) and dried at 60  $^{\circ}\text{C}$ .

**Procedure for the photocatalytic aerobic oxidation of 1a with scavengers.** Under air atmosphere, **1a** (0.10 mmol), scavengers (0.1 mmol, 0.5 mmol was used for the TBA, 5 mol% was used for TEMPO) and photocatalyst **CMP-NHPI** (4.0 mg) in 0.5 mL of solvent were stirred at room temperature with the irradiation of white LED lamp (400–830 nm, 20 W). (1) After the reaction in MeCN was completed, the insoluble material was removed by centrifugation. The conversion (Con.) and selectivity (Sel.) were checked by GC–MS analysis using naphthalene as the internal standard. (2) After the reaction in H<sub>2</sub>O was completed, a small amount of ethyl acetate was added into the reaction mixture. After the insoluble material was removed by centrifugation, the resulting solution was extracted by ethyl acetate and the combined organic phase was dried over anhydrous MgSO<sub>4</sub>. The conversion (Con.) and

selectivity (Sel.) were checked by GC–MS analysis using naphthalene as the internal standard.

### **EPR Detection of Reactive Oxygen Species**

**For detection of  $^1\text{O}_2$ .** Typically, 2,2,6,6-tetramethylpiperidine (TEMP, 100 mM, 50  $\mu\text{L}$ ) was added to the suspension of **CMP-NHPI** (2.0 mg) in MeCN or  $\text{H}_2\text{O}$  (0.2 mL). And then EPR measurements were carried out at room temperature in the dark or under LED lamp (400–830 nm, 20W).

**For detection of  $\text{O}_2^{\cdot-}$ .** Typically, 5,5-dimethyl-1-pyrroline N-oxide (DMPO, 100 mM, 30  $\mu\text{L}$ ) was added to the suspension of **CMP-NHPI** (2.0 mg) in MeCN or  $\text{H}_2\text{O}$  (0.2 mL). And then EPR measurements were carried out at room temperature in the dark or under LED lamp (400–830 nm, 20W).

**Detection Procedure of  $\text{H}_2\text{O}_2$** <sup>[2]</sup>. Under air atmosphere, **1a** (0.10 mmol) and photocatalyst **CMP-NHPI** (4.0 mg) in 0.5 mL of solvent were stirred at room temperature with the irradiation of white LED lamp (400–830 nm, 20 W). After the reaction was completed, the reaction mixture was filtrated by a 0.22  $\mu\text{m}$  filter to remove the insoluble solids. And then the saturated titanium sulfate solution was added to the filtrate. The color of the solution immediately changed from colorless to yellowish brown upon the addition of the titanium sulfate solution. Subsequently the absorbance of the obtained solution was checked by UV–vis spectrophotometer.

The control experiment was carried out under the same condition without the addition of **1a**. After the saturated titanium sulfate solution was added, the color of the filtrate remained unchanged.

### 3. Figures and tables

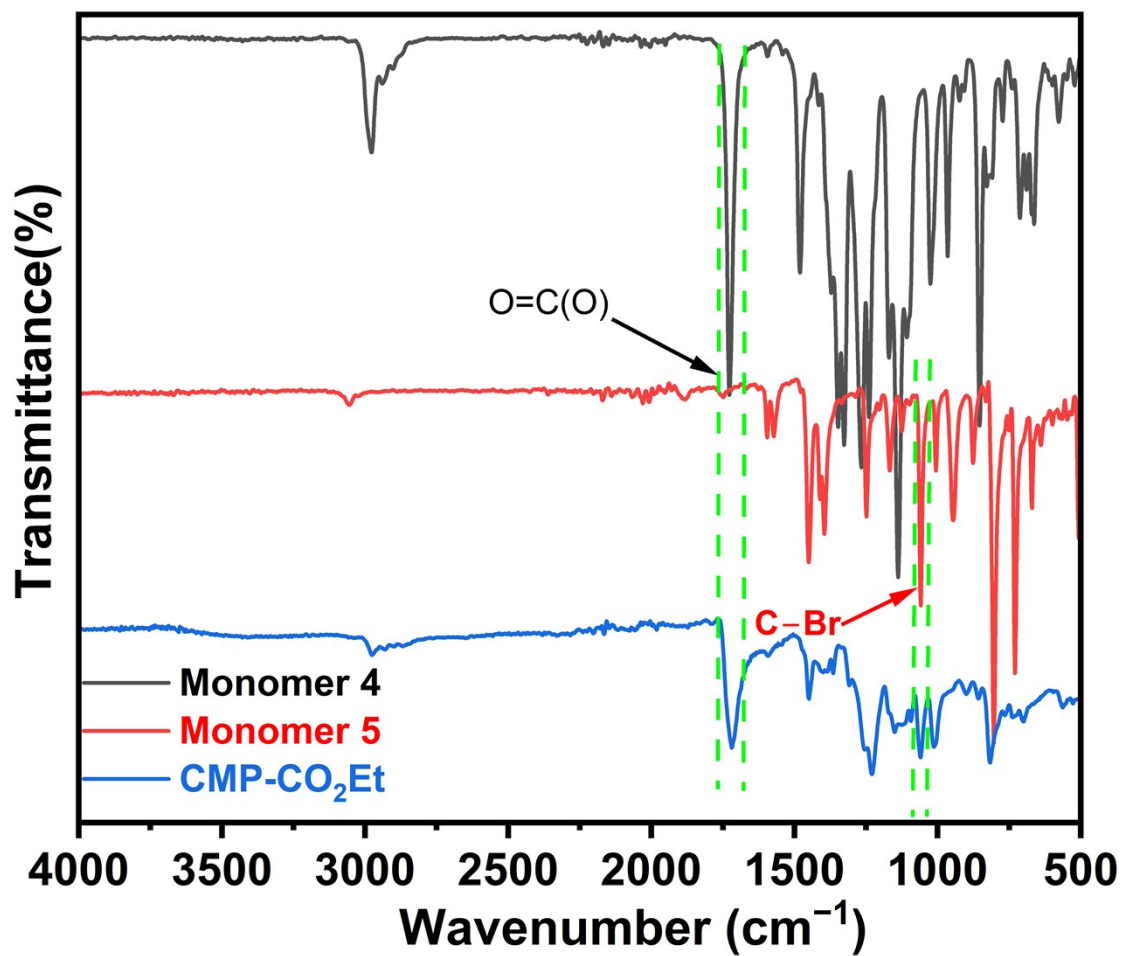
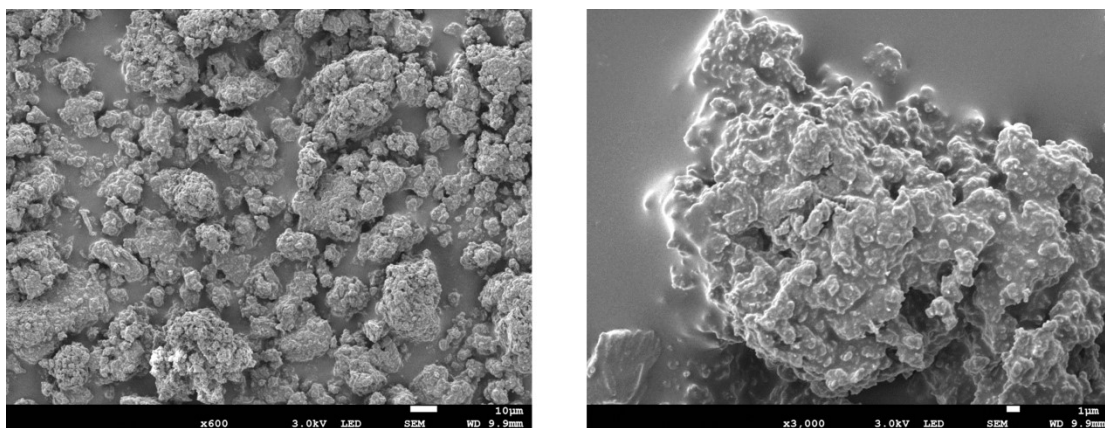
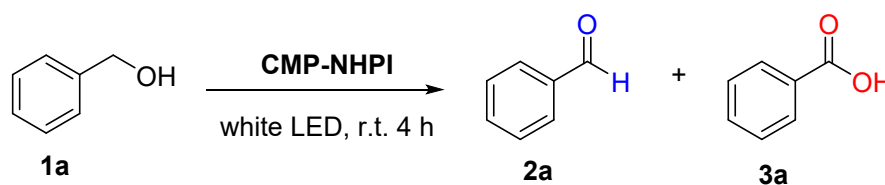


Figure S1. FT-IR spectra of 4 (black), 5 (red) and the CMP-CO<sub>2</sub>Et (blue).



**Figure S2.** SEM images of the CMP-NHPI.

**Table S1.** Catalytic oxidation of benzyl alcohol under different solvents<sup>a, b</sup>



Entry	Photocatalyst	Solvent	Conv.	Sel.	
				<b>2a</b>	<b>3a</b>
1	<b>CMP-NHPI</b>	MeCN	98	>99	trace
2	<b>CMP-NHPI</b>	DCE	3	100	0
3	<b>CMP-NHPI</b>	Dioxane	3	100	0
4	<b>CMP-NHPI</b>	DMSO	47	100	3
5 <sup>c</sup>	–	MeCN	3	100	0

<sup>a</sup> Reaction conditions: **1a** (0.1 mmol), photocatalyst (4 mg), solvent (0.5 mL), white LED (20 W), air (1 atm). <sup>b</sup> Determined by GC. <sup>c</sup> 30% H<sub>2</sub>O<sub>2</sub> (50 ul). DCE: 1,2-dichloroethane.

**Table S2.** Photocatalytic performance comparison of representative heterogeneous photocatalysts for the selective oxidation of benzyl alcohol.

Photocatalyst	Time (h)	Gas	Product	Conv. (%)	Sel. (%)	Yield <sup>a</sup> (%)	Ref.
<b>CMP-NHPI</b>	4	Air	CHO	98	98	96	This work
	5	Air	COOH	100	99	99	
<b>Zr<sub>6</sub>-Cu/Fe-1</b>	48	O <sub>2</sub>	CHO	-	-	80	3
<b>CN photoanode</b>	58	O <sub>2</sub>	COOH	-	-	99	4
<b>CNNA</b>	9	O <sub>2</sub>	CHO	68.3	99	68	5
<b>MelonHP</b>	24	O <sub>2</sub>	CHO	36	99		6
<b>mpg-C<sub>3</sub>N<sub>4</sub><sup>b</sup></b>	3	O <sub>2</sub> (8 bar)	CHO	57	99	57	7
<b>MIL-125/Ag/g-C<sub>3</sub>N<sub>4</sub></b>	6	O <sub>2</sub>	CHO	65	98	64	8
<b>MCN-A<sup>c</sup></b>	3	O <sub>2</sub> (1 bar)	CHO	53	99	53	9
<b>TCNg<sup>d</sup></b>	4	O <sub>2</sub>	CHO	72	100	72	10
<b>COF/CdS</b>	15	O <sub>2</sub>	CHO	97.1	99.9	97	11
<b>Pt/PCN-224(Zn)</b>	0.8	O <sub>2</sub>	CHO	99	100	99	12
<b>PCN-224(Sb)-OH</b>	8	O <sub>2</sub>	CHO	93	100	93	13
<b>Bi-TATB</b>	5	O <sub>2</sub>	CHO	37.25	100	37.25	14
<b>CTH-TH@SBA-15</b>	4	O <sub>2</sub>	CHO	99	99	99	15
<b>TiO<sub>2</sub>/AA/Co/NHPI<sup>e</sup></b>	0.25	air	CHO	85	99	85	16
<b>Co-g-C<sub>3</sub>N<sub>4</sub>-imine/TiO<sub>2</sub>/NHPI<sup>f</sup></b>	1.5	air	CHO	98	99	98	17
<b>mpg-C<sub>3</sub>N<sub>4</sub>/NHPI</b>	28	O <sub>2</sub>	CHO	85	82	70	18

<sup>a</sup> Yield = Conv. × Sel. <sup>b</sup> 100 °C. <sup>c</sup> 60 °C. <sup>d</sup> 50 °C. <sup>e</sup> 70 °C. <sup>f</sup> 70 °C.

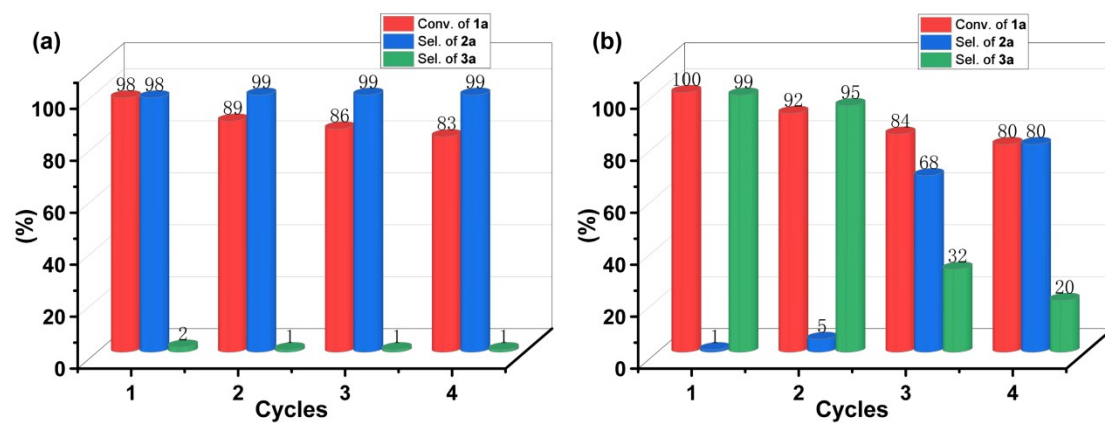


**Figure S3.** The recycling tests of benzyl alcohol oxidation in (a) MeCN and (b) H<sub>2</sub>O catalyzed by the **CMP-NHPI**.

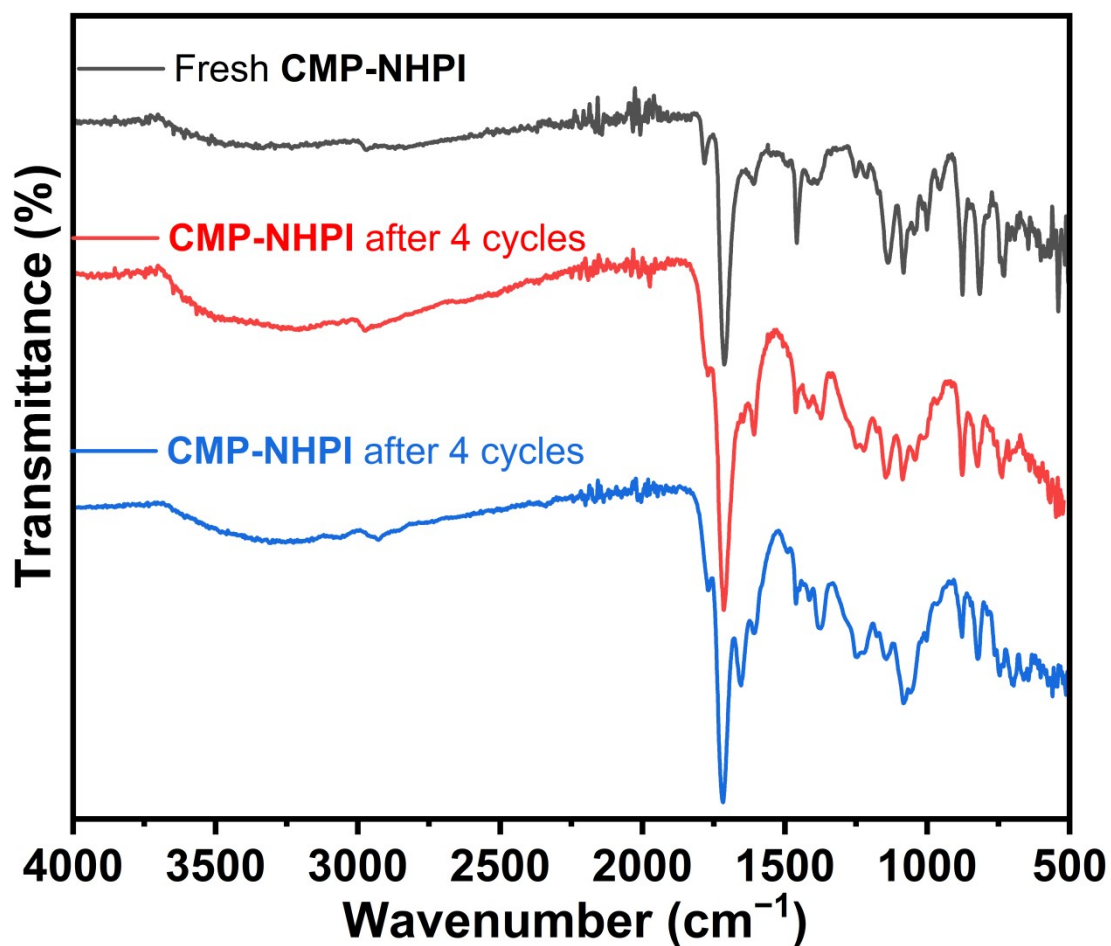


**Figure S4.** FT-IR spectra of the **CMP-NHPI** before and after the catalytic oxidation of benzyl alcohol (red: in MeCN; blue: in H<sub>2</sub>O).

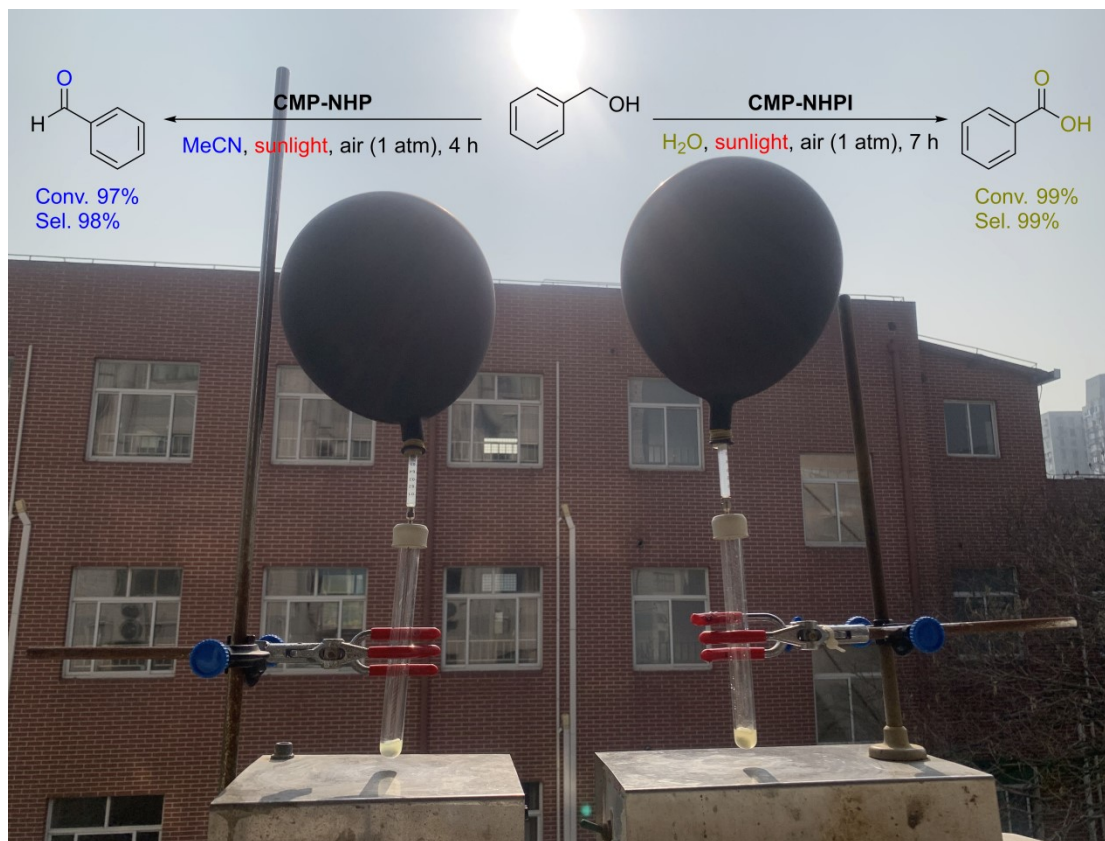


**Figure S5.** The photo of catalytic oxidation of the benzyl alcohol carried out under the natural sunlight in Shanghai, China (12/14/2023–12/14/2023, temperature: *ca.* 20–22 °C)

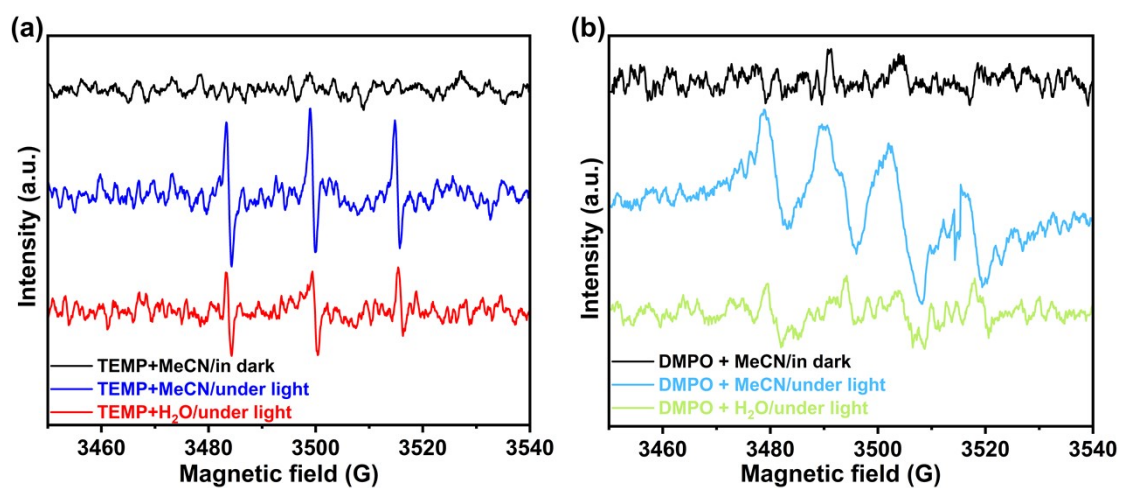


**Figure S6.** The detected EPR signals of  $^1\text{O}_2$  trapped by (a) TEMP and  $\text{O}_2^{\bullet-}$  trapped by (b) DMPO in MeCN and  $\text{H}_2\text{O}$ , respectively.

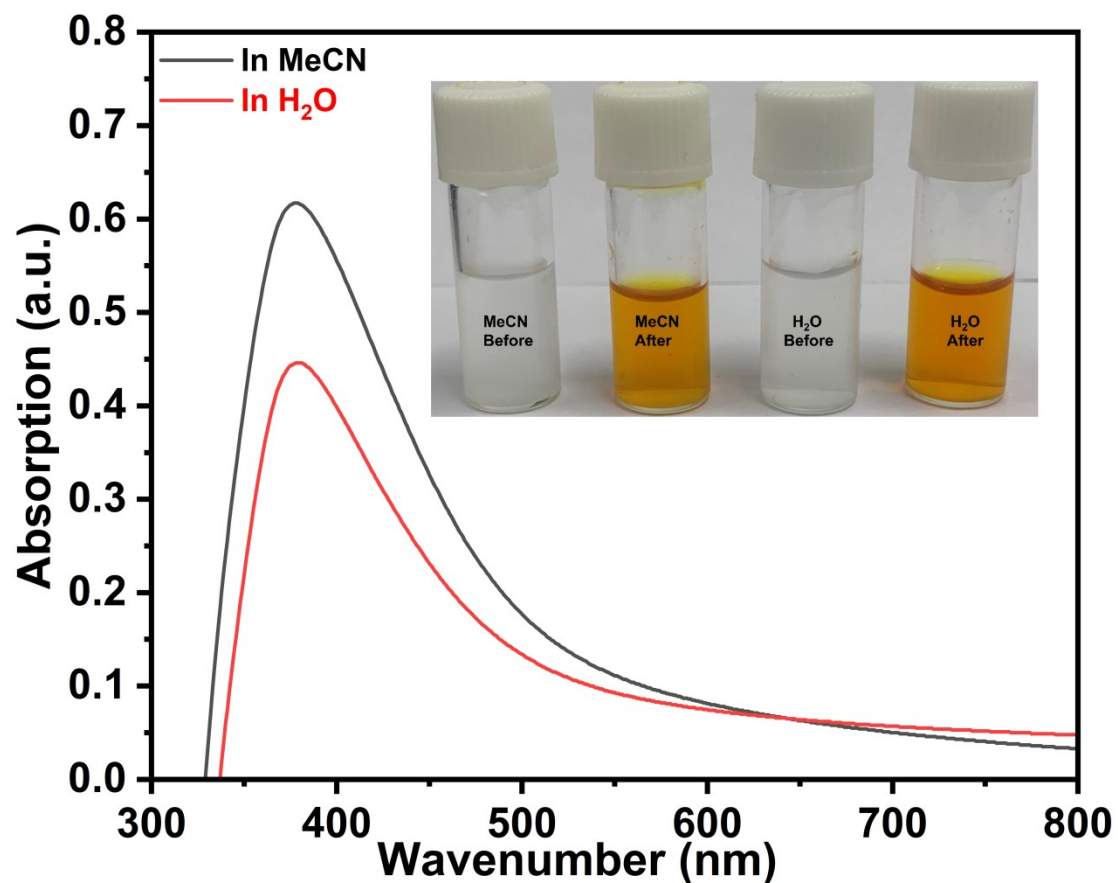


**Figure S7.** UV-Vis absorption spectra of the photocatalytic reaction solution treated by the titanium sulfate colorimetric method. In MeCN (black). In H<sub>2</sub>O (red). (Inset: The color change before and after the addition of titanium sulfate solution).

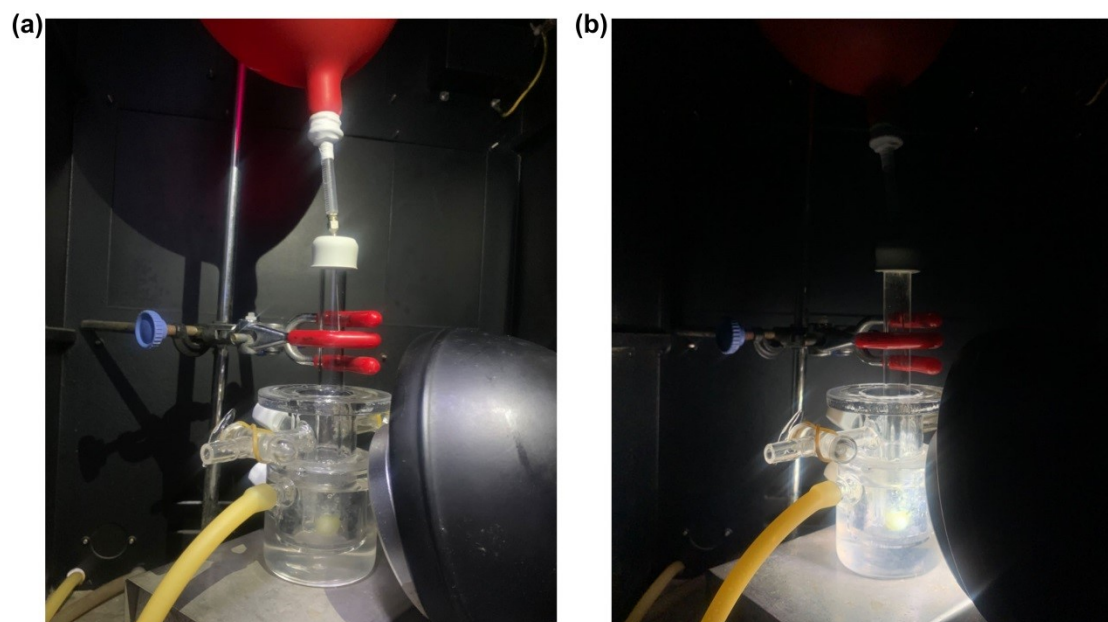


**Figure S8.** The experimental setups of the photocatalytic aerobic oxidation with the (a) light off and (b) light on.

#### 4. References

- [1] T. Fan, M. Wang, Y. Yin, L. Fang, H. Xu, G. Wu, L. Li, Porous Aromatic Framework Covalently Embedded with *N*-Hydroxyphthalimide as Metal-free Heterogeneous Catalyst for Highly Efficient and Selective Aerobic Oxidation, *ChemCatChem*, 2024, **16**, e202301171.
- [2] J.-Y. Yue, L.-P. Song, Y.-F. Fan, Z.-X. Pan, P. Yang, Y. Ma, Q. Xu, B. Tang, Thiophene-Containing Covalent Organic Frameworks for Overall Photocatalytic H<sub>2</sub>O<sub>2</sub> Synthesis in Water and Seawater, *Angew. Chem. Int. Ed.*, 2023, **62**, e202309624.
- [3] X. Feng, Y. Pi, Y. Song, Z. Xu, Z. Li, W. Lin, Integration of Earth-Abundant Photosensitizers and Catalysts in Metal–Organic Frameworks Enhances Photocatalytic Aerobic Oxidation, *ACS Catal.*, 2021, **11**, 1024–1032.
- [4] N. Karjule, R.S. Phatake, S. Barzilai, B. Mondal, A. Azoulay, A.I. Shames, M. Volokh, J. Albero, H. García, M. Shalom, Photoelectrochemical alcohols

- oxidation over polymeric carbon nitride photoanodes with simultaneous H<sub>2</sub> production, *J. Mater. Chem. A*, 2022, **10**, 16585–16594.
- [5] J. Ding, W. Xu, H. Wan, D. Yuan, C. Chen, L. Wang, G. Guan, W.-L. Dai, Nitrogen vacancy engineered graphitic C<sub>3</sub>N<sub>4</sub>-based polymers for photocatalytic oxidation of aromatic alcohols to aldehydes, *Appl. Catal., B*, 2018, **221**, 626–634.
- [6] W. Zhang, C. Xu, T. Kobayashi, Y. Zhong, Z. Guo, H. Zhan, M. Pruski, W. Huang, Hydrazone-Linked Heptazine Polymeric Carbon Nitrides for Synergistic Visible-Light-Driven Catalysis, *Chem.–Eur. J.*, 2020, **26**, 7358–7364.
- [7] F. Su, S.C. Mathew, G. Lipner, X. Fu, M. Antonietti, S. Blechert, X. Wang, mpg-C<sub>3</sub>N<sub>4</sub>-Catalyzed Selective Oxidation of Alcohols Using O<sub>2</sub> and Visible Light, *J. Am. Chem. Soc.*, 2010, **132**, 16299–16301.
- [8] Z. Yang, X. Xu, X. Liang, C. Lei, Y. Cui, W. Wu, Y. Yang, Z. Zhang, Z. Lei, Construction of heterostructured MIL-125/Ag/g-C<sub>3</sub>N<sub>4</sub> nanocomposite as an efficient bifunctional visible light photocatalyst for the organic oxidation and reduction reactions, *Appl. Catal., B*, 2017, **205**, 42–54.
- [9] Y. Chen, J. Zhang, M. Zhang, X. Wang, Molecular and textural engineering of conjugated carbon nitride catalysts for selective oxidation of alcohols with visible light, *Chem. Sci.*, 2013, **4**, 3244–3248.
- [10] M. Mohammadi, H. Hadadzadeh, M. Kaikhosravi, H. Farrokhpour, J. Shakeri, Selective Photocatalytic Oxidation of Benzyl Alcohol at Ambient Conditions using Spray-Dried g-C<sub>3</sub>N<sub>4</sub>/TiO<sub>2</sub> Granules, *Mol. Catal.*, 2020, **490**, 110927.
- [11] K. Zhang, G. Lu, Z. Xi, Y. Li, Q. Luan, X. Huang, Covalent organic framework stabilized CdS nanoparticles as efficient visible-light-driven photocatalysts for selective oxidation of aromatic alcohols, *Chin. Chem. Lett.*, 2021, **32**, 2207–2211.
- [12] Y.-Z. Chen, Z.U. Wang, H. Wang, J. Lu, S.-H. Yu, H.-L. Jiang, Singlet Oxygen-Engaged Selective Photo-Oxidation over Pt Nanocrystals/Porphyrinic MOF: The Roles of Photothermal Effect and Pt Electronic State, *J. Am. Chem. Soc.*, 2017, **139**, 2035–2044.
- [13] D. Xie, S. Li, W. Yang, S. Fan, Y.-S. Feng, Selective Photocatalytic Conversion

- of Benzyl Alcohol to Benzaldehyde by Antimony(V) Porphyrin Metal-Organic Frameworks under Visible-Light Irradiation, *ChemistrySelect*, 2022, **7**, e202103521.
- [14] R. Zhang, Y. Liu, Z. Wang, P. Wang, Z. Zheng, X. Qin, X. Zhang, Y. Dai, M.-H. Whangbo, B. Huang, Selective photocatalytic conversion of alcohol to aldehydes by singlet oxygen over Bi-based metal-organic frameworks under UV–vis light irradiation, *Appl. Catal., B*, 2019, **254**, 463–470.
- [15] W. Huang, B.C. Ma, H. Lu, R. Li, L. Wang, K. Landfester, K.A.I. Zhang, Visible-Light-Promoted Selective Oxidation of Alcohols Using a Covalent Triazine Framework, *ACS Catal.*, 2017, **7**, 5438–5442.
- [16] M. Jafarpour, F. Feizpour, A. Rezaeifard, Aerobic benzylic C–H oxidation catalyzed by a titania-based organic–inorganic nanohybrid, *RSC Adv.*, 2016, **6**, 54649–54660.
- [17] N. Pourmorteza, M. Jafarpour, F. Feizpour, A. Rezaeifard, TiO<sub>2</sub> nanoparticles decorated with Co-Schiff baseg-C<sub>3</sub>N<sub>4</sub> as an efficient photocatalyst for one-pot visible light-assisted synthesis of benzimidazoles, *RSC Adv.*, 2022, **12**, 22526–22541.
- [18] P. Zhang, J. Deng, J. Mao, H. Li, Y. Wang, Selective aerobic oxidation of alcohols by a mesoporous graphitic carbon nitride/*N*-hydroxyphthalimide system under visible-light illumination at room temperature, *Chin. J. Catal.*, 2015, **36**, 1580–1586.